BULLETIN OF THE EARTHQUAKE
RESEARCH INSTITUTE
UNIVERSITY OF TOKYO
Vol. 59 (1984) pp. 467-500

Distribution of Ground-Motion Amplification Factors as a Function of Period (3-15 sec), in Japan

Ljubica MAMULA*, Kazuyoshi KUDO and Etsuzo SHIMA

Earthquake Research Institute, University of Tokyo

(Received October 31, 1984)

Abstract

The increasing number of structures with long natural periods (between 3 sec and 15 sec) makes it necessary to study the strong-motion characteristics in this period range. The damping coefficient of these objects is small and it may cause serious damage at the resonance period. The authors propose the method for estimating the site amplification factors in terms of period by analyzing the large number of strong-motion displacement records of the Kita-Mino earthquake of August 19, 1961, Japan. The observed spectra corrected for the geometrical spreading of surface waves and attenuation factor were compared with the synthetic spectra computed utilizing the normal mode solution. Good agreement was obtained between observations and synthetics at the stations close to the epicenter which are located on the standard crustal structure, so that the difference between the observed and synthetic spectral amplitudes at the other stations reflect the site amplification factor. The site amplification factor, ratios of observed spectra to synthetics, distribute from 0.3 to 14. At certain sites, they strongly depend on period.

Introduction

Understanding the nature of 2 sec to 20 sec strong ground motion has become important for the anti-seismic design of structures, such as big oil tanks, long-span bridges, high-rise buildings, etc., since they have a natural period within this range. Considering their economical convenience, the number of these structures will increase in the future, following the growth of industry and rapid urbanization.

It is known that both short and long-period strong-motions caused by

* On leave from Seismological Institute Beograd, Yugoslavia.

earthquakes contribute to the damage of structures, but the damage due only to long-period ground motion has hardly been observed. However, during the Nihonkai-Chubu earthquake (May 26, 1983, $M=7.9$), oil sloshed from the big tanks in Niigata, even though the maximum acceleration was less than 15 cm/sec^2, i.e., short-period motion was not significant. As far as we know, it would be the first experience of only long-period earthquake motion bringing about the damage. KUDO and SAKAUE (1984) suggested that the long-period motion was predominant due to the presence of thick, soft sediments at Niigata.

Although the nature of long-period earthquake ground motion is essentially related to the earthquake source process (OHTA and KAGAMI, 1976), the site effect plays an important role, as will be discussed in this paper.

OKADA and KAGAMI (1978) determined the amplitude amplification at the site in Japan for long-period waves (1–10 sec) by treating statistically maximum amplitudes of the large number of shallow earthquakes ($h<60$ km, $5.4<M$). Their results give an average amplitude amplification at the specific site but they did not give sufficient information in terms of period or frequency. The determination of the shakeability at the site as a function of periods is keenly required, especially for the purpose of anti-seismic design of long-period structures because of its small damping or high resonance at the natural period. In other words, a long period structure has strong selectivity on period or frequency.

It has been recognized that the long-period strong motion is mainly composed of surface waves (TRIFUNAC and BRUNE, 1970; HASEGAWA, 1974; HANKS, 1975; HERRMANN and NUTTLI, 1975a, b; SWANGER and BOORE, 1978a, b; KUDO, 1978, 1980) and that the superposition of normal modes well approximates the theoretical complete solution (KAWASAKI, 1978; SWANGER and BOORE 1978a, b; HERRMANN, 1979).

Generally speaking, the focal depth of earthquakes which cause severe damage is shallow, therefore it is reasonable to assume that surface waves predominate in the strong ground motion. The excitation of surface waves is controlled by the underground structure so that, if it is known, the amplitude amplification factor at the site can be estimated. However, both shallow and deep underground structures are known in only a few areas, so we have to turn to some other methods for determining the site amplification factor for the whole area of Japan. By analyzing sufficiently large number of data from one earthquake, we will try to estimate the site amplitude amplification factors in the period range from 3 sec to 15 sec. In order to extract the site amplification factor from observations, the

effect of the source radiation on the observed amplitudes was excluded assuming the observed waves were composed of surface waves.

Data

The strong-motion seismograms of the Kita-Mino earthquake of August 19, 1961, were analysed. The epicenter of the earthquake was located near Haku-san in Central Honshu, Japan. The 45 displacement records of the JMA network over Honshu and Kyushu were available. The natural period (To), the damping constant (h) and the static magnification (V) of the strong-motion seismographs are 5–6 sec, 0.5–0.6 and 1, respectively. Fortunately, seismograph constants were well determined, thus we could perform the instrumental response correction. The digitization of the provided data

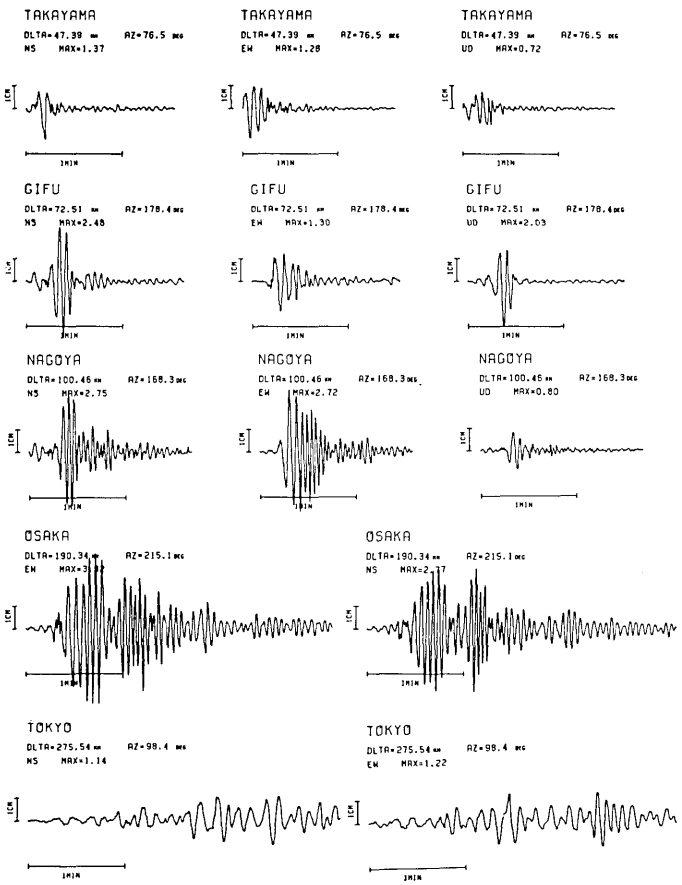

Fig. 1. An example of JMA strong-motion records of the Kita-Mino earthquake (August, 1961) showing the significance of the site effect on seismic wave amplitude and period.

was conducted by H. Kawasumi and arranged for the computational convenience by SATÔ and SHIMA (1978). The digitization was conducted at the interval of 0.2 sec and the arc correction was performed. The waveforms are shown in Appendix I.

As an example, the observed seismograms at different epicentral distances are shown in Fig. 1. The first thing to notice is that the observed amplitudes increase with the epicentral distance and the long-period waves predominate at Tokyo. This suggests that the local effect on seismic waves is significant. The sites such as Nagoya, Osaka and Tokyo are the sites where thick alluvial or diluvial deposits are found. With this in mind, it is our intention to determine the amplitude amplifications at such locations.

In order to determine the amplification factors at the locations where the strong-motion records were available, we divided our work into two steps:

In the first step, the amplitude amplification factors at the site were obtained for the observed values.

In the second step, we determined the amplitude amplifications at these sites after eliminating the effect of the source by comparing theoretical and observed amplitudes corrected for the distance and attenuation coefficient, as is presented in Fig. 2.

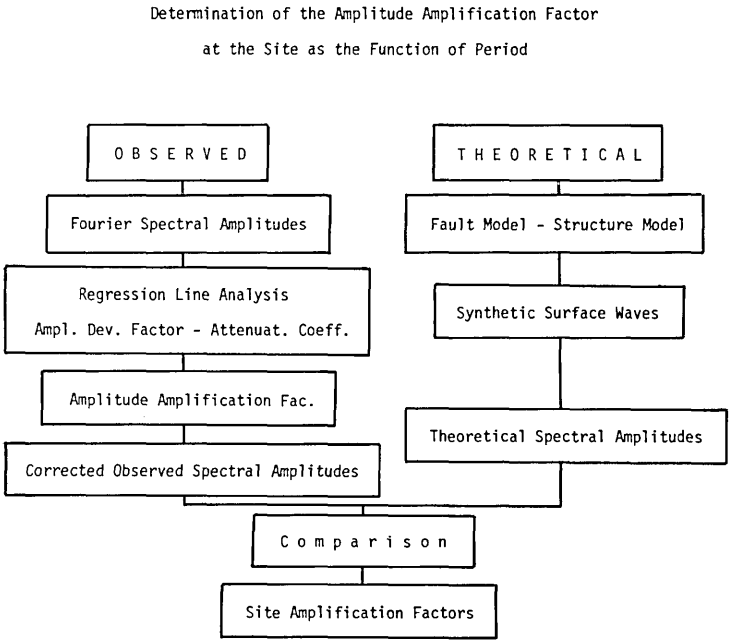

Fig. 2. Flowchart of the analysis.

Spectra

The spectral amplitudes were computed using the FFT method and the standard Hanning window was applied. The instrumental response was removed and the results are shown in Appendix II. At some stations prominent peaks were found at certain periods. For example, at Nagoya ($r=100$ km) or Osaka ($r=190$ km), the extremely high values were registered at periods of 3 sec and 4-5 sec, respectively, almost 10 times larger than the amplitudes at Takayama ($r=47$ km). At Tokyo, however, the maximum amplitude was observed at 10 sec. Considering the damage caused to the oil plant during the Nihonkai-Chubu earthquake, it would be interesting to obtain the amplification factor at Niigata but, unfortunately, the seismogram was not available.

Attenuation

The amplitude amplification factor at the site for different periods in case of the Kita-Mino earthquake was obtained as the spectral amplitude deviation from the standard attenuation curve determined by regression line analysis, in the following manner.

Considering the fact that the focus of the Kita-Mino earthquake was shallow ($h=2$ km, KAWASAKI, 1978) the observed waves should be mainly composed of surface waves, we assumed geometrical spreading for surface waves and the following form of the amplitudedistance dependence:

$$A=A' \exp(-\alpha r)/\sqrt{r}$$

where A=amplitude spectrum; A'=constant; r=epicentral distance and α=attenuation coefficient.

In general, the attenuation coefficients of Rayleigh and Love waves would not be the same. However, our aim is not to obtain the exact attenuation coefficients but to determine the site amplification factor. For simplicity, the square root of the sum of the power spectra of two horizontal components is used as the spectral amplitude at the site. The data on both horizontal components were available for 39 stations. Vertical component was excluded from the analysis because it was missing at some stations and it is less significant than the horizontal ones from the engineering point of view.

After performing correction for geometrical spreading, the spectral amplitudes vs. epicentral distances were plotted for every period from

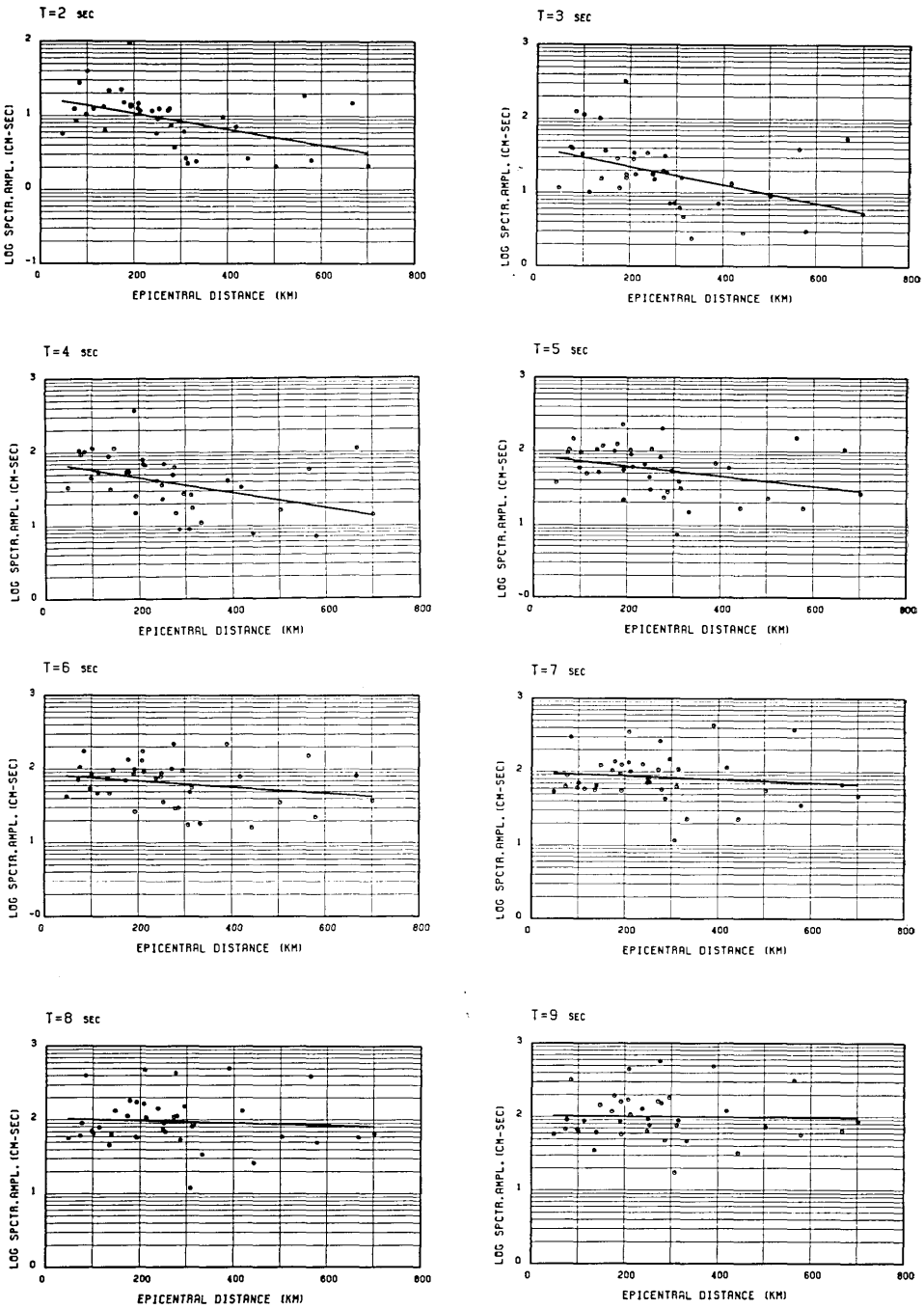

Fig. 3(a). Observed spectral amplitudes corrected for geometrical spreading vs. epicentral distance, as a function of period. The straight lines are determined by regression line analysis.

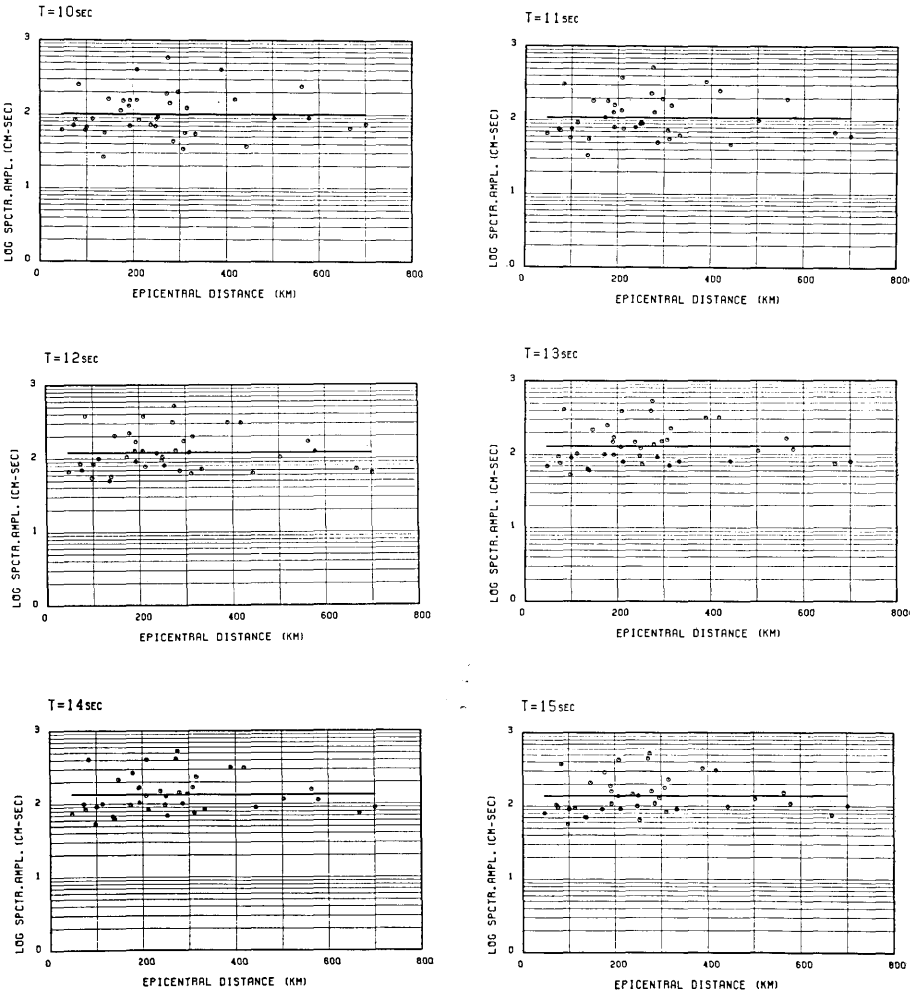

Fig. 3(b)

3 sec to 15 sec, as is shown in Fig. 3. The straight lines determined by regression line analysis give an average value at a distance and the inclination of the line gives the apparent attenuation coefficient. The deviation from the average represents the shakeability at the site. Large deviations are found at Nagoya, Osaka, Saga and Oita in the period range from 3 sec to 5 sec and at Tokyo on periods longer than 7 sec.

The ratios of observed amplitudes to their average with respect to epicentral distances were classified into 6 classes. They are: less than 0.38; between 0.38 and 0.75; between 0.75 and 1.5 (standard); between 1.5 and 3; between 3 and 6; greater than 6. Thus classified amplitude amplification factors are plotted on the maps and are shown in Fig. 4 at periods of 3 sec

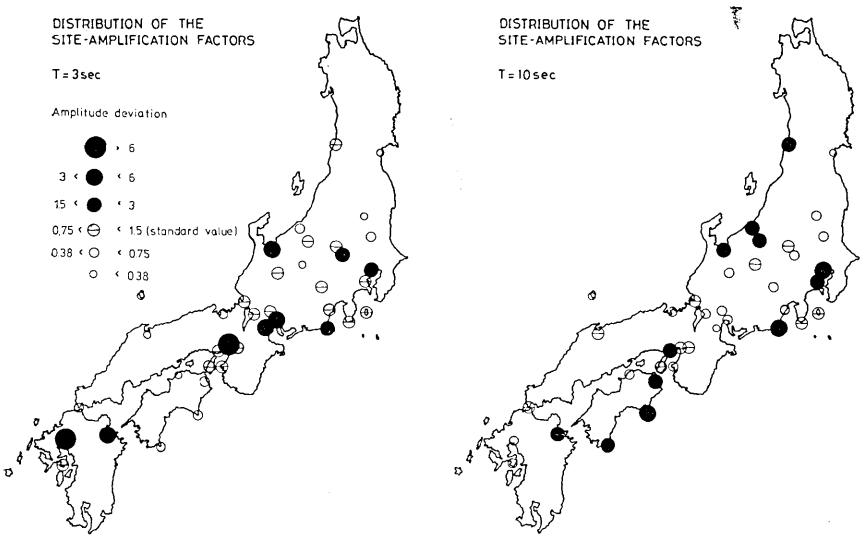

Fig. 4. The apparent site amplification factor determined from the observed data at different periods (3 sec and 10 sec).

and 10 sec. The first thing to notice is that the amplitude amplification factors of adjacent sites differ more than 2 classes. For example, the factor of Osaka is 6 times greater than the ones of Nara and Kobe at a period of 3 sec.

If one compares the values obtained for different periods at the same site, the dependence of the amplitude amplification on the period is apparent. In the case of Osaka, the amplification factors determined for the periods of 3 sec and 10 sec differ more than two classes. The big difference is also observed at Tokyo, Yokohama, Nagoya and Saga.

Therefore, it can be concluded that the amplitude amplification factor at the one and the same site depends greatly on the period. However, as the amplitude of ground motion depends not only on site conditions, but also on the radiation pattern of the source and the propagation path, the above results give us a rather rough understanding of the shakeability at the site. If we analyse the data of a number of earthquakes similar to these discussed in the present paper, it would be possible to determine the amplitude factors at the sites as an average, disregarding the source effect. As it is still a rare case to find such a multitude of applicable data, we attempted to solve the problem by eliminating the source effect from the results.

Synthetics

In order to eliminate the source effects from the observations, both source and structure models were reexamined with the results of KAWASAKI (1975) as the basis. Using seismic and geodetic data, he obtained the fault model of the Kita-Mino earthquake as is shown in Table 1. To deduce the fault model, he compared the synthetic waves computed from the complete solution for semi-infinite medium with the strong-motion displacement records and obtained a good matching in the portion of the earlier arrivals of S-wave first cycle. However, his approach may underestimate the observations at the later arrivals. This is caused by the disregard of vertical heterogeneities of the surface structure. Therefore, dispersive surface waves should be taken into account.

Far-field spectral amplitudes of horizontal Love and Rayleigh waves for a point double couple force can be written as (HARKRIDER, 1970),

$$\boldsymbol{U}(\omega)=\boldsymbol{S}(\omega)k\boldsymbol{X}(\theta, h)\boldsymbol{E}\exp[-i(kr+3\pi/4)]/\sqrt{2\pi r}$$

where $\boldsymbol{S}(\omega)$=spectral source function; $\boldsymbol{X}(\theta, h)$=radiation pattern function; $\boldsymbol{E}=\varepsilon_0 A_R k^{-1/2}$ for Rayleigh waves and $\boldsymbol{E}=A_L k^{-1/2}$ for Love waves; ε_0=surface elipticity; A_R and A_L=amplitude responses of Rayleigh and Love waves; k=Love or Rayleigh wavenumber; θ=azimuthal angle measured counterclockwise from the strike direction to the station; h=focal depth and r=epicentral distance.

Table 1. Fault-Model of the Kita-Mino earthquake of August 19, 1961 (KAWASAKI, 1975).

Fault	the Hatogayu-Koike Fault
Origin time	1961, Aug. 19, 14h 33 m 32.8 sec (JST)
Epicenter	E136°44′, N36°05′
Focal depth	2 km
Fault plane	Dip direction N55°W
	Dip angle 60°
Slip angle of hanging wall	130° (Right lateral, reverse)
Fault length	12 km
Fault width	10 km
Rupture velocity	3.0 km/sec : Unilateral
Average dislocation	2.5 m
Rise time	2 sec
Velocity of fault motion	60 cm/sec
Seismic moment	0.9×10^{26} dyne. cm
Stress drop	160 bars
Strain energy released	1.7×10^{22} ergs

Synthetic seismograms were obtained by the inverse Fourier transform. Three stations, Takayama, Gifu and Tsuruga were chosen for the comparison between observations and synthetics to verify the source model and to determine the standard structure model. These stations were con-

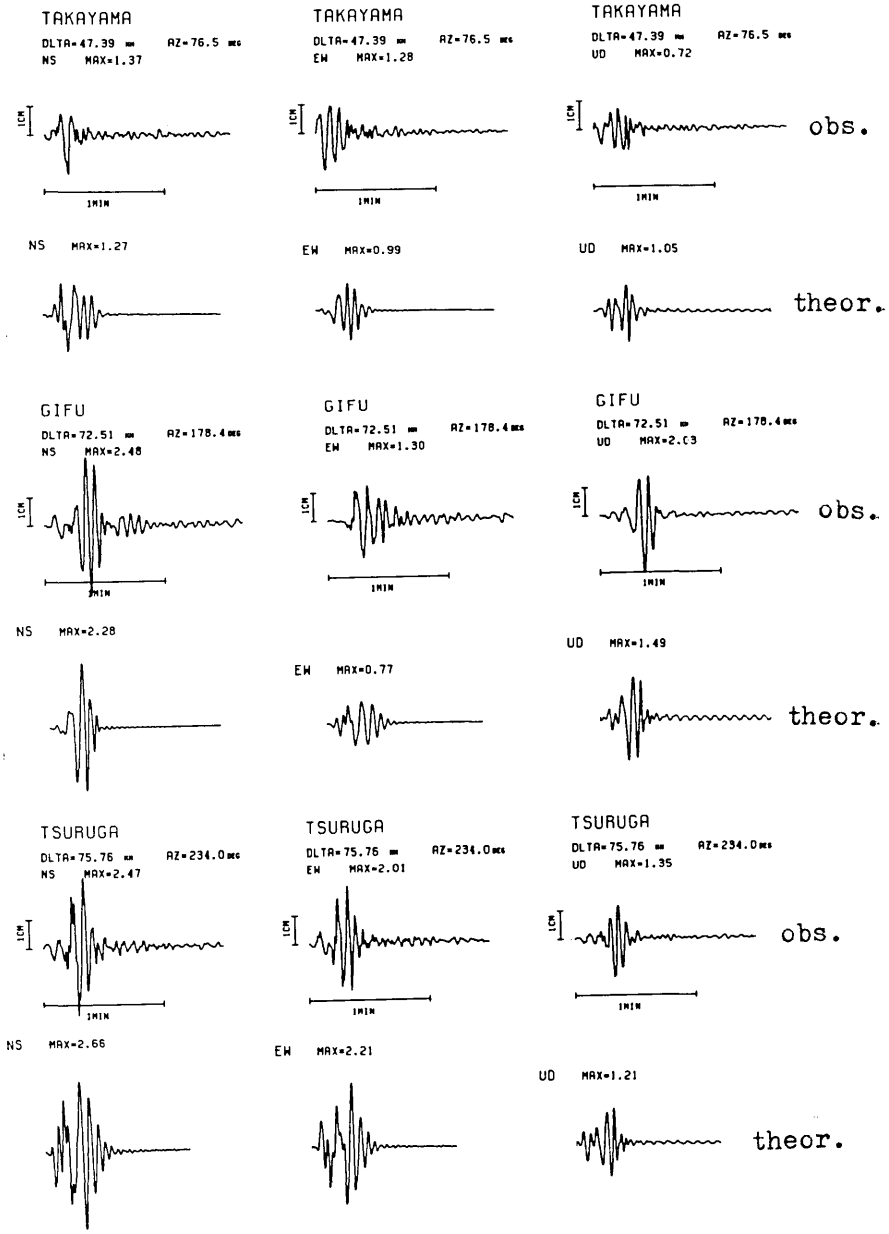

Fig. 5. Comparison between synthetic and observed seismograms at Takayama, Gifu and Tsuruga.

venient for checking the radiation pattern or the source model as they surround the epicenter and their site amplification factors were close to the standard determined by OKADA and KAGAMI (1978). In the computation of synthetic seismograms, a cosine-taper band-pass filter (0.017–0.5 Hz) was applied in frequency domain and the seismograph correction was also performed. The best matching between the observations and synthetics was obtained when the unilateral rupture mode of Kawasaki's model was changed into a bilateral one, L_1 (north-east portion)=4 km and L_2 (south-west)=8 km. It was not necessary to modify the other fault parameters. The appropriate structure model is shown in Table 2 where the low-velocity layers cover the crustal structure. A similar structure model is given by KUDO et al. (1978).

The synthetic seismograms at Takayama, Gifu and Tsuruga were compared with the observed ones (Fig. 5). The

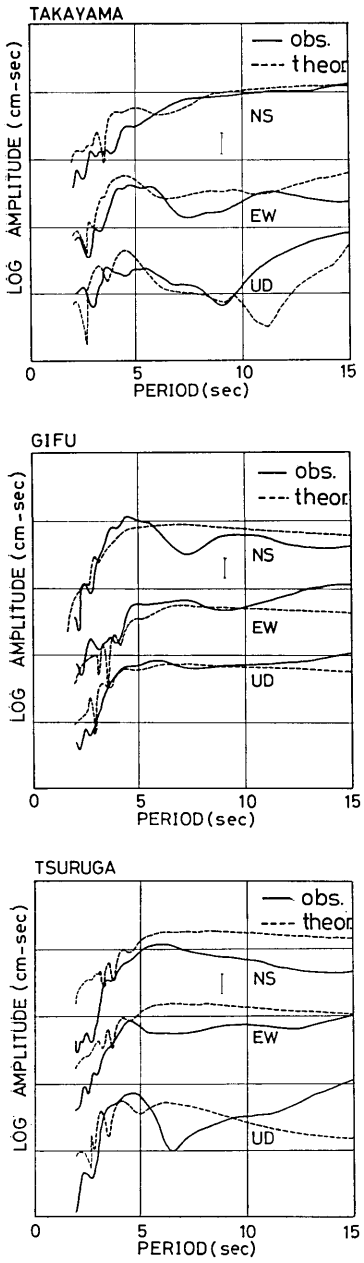

Fig. 6. Comparison between theoretical and observed spectral amplitudes at Takayama, Gifu and Tsuruga. A vertical bar shows the two time difference.

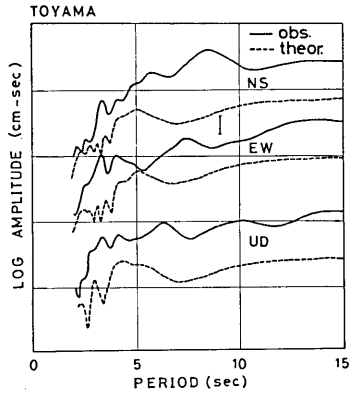

Fig. 7. Synthetic and observed spectral amplitudes at Toyama, showing apparent differences that suggest the presence of thick sedimentary layers at the site.

Table 2. Structure model adopted for the computation of synthetic surface waves.

No Layer	Vp (km/sec)	Vs (km/sec)	Density (g/cm^3)	H (km)
1	3.5	1.5	2.2	1.0
2	4.5	2.5	2.3	1.0
3	5.5	3.0	2.5	3.0
4	6.0	3.7	2.8	15.0
5	6.8	3.9	3.0	10.0
6	8.0	4.3	3.3	∞

synthetic and observed spectral amplitudes are shown in Fig. 6. The matching between synthetic and observed waveforms for the stations selected as standard was fair, i.e., the synthetic spectra did not differ more than twice from the observations, roughly speaking. This can be considered as satisfactory. In Fig. 7, the observed and synthetic amplitude spectra at Toyama were presented as an example of poor matching, suggesting thick sedimentary layers at the site.

Determination of the Amplitude Factor at the Site

As we have seen, both source and site significantly influence the observed waves. In order to exclude the source effect from the observations, as a first step, the waves should be equalized to a certain distance. For this purpose, the attenuation coefficient has to be taken into account. Previously determined attenuation coefficients (using all data) were strongly influenced by the deviated values and they do not necessarily reflect the standard attenuation. Therefore, we redetermined the attenuation coefficient as a function of period excluding the data that deviate more than 3 times or less than 0.38 times from the standard attenuation curve, as well as the data at epicentral distances less than 100 km. Attenuation coefficients thus obtained are shown in Table 3. CHENG and MITCHELL (1981) obtained similar values of attenuation coefficients in the USA using Rayleigh waves. Although our result is obtained from a rather rough analysis, it is interesting to note that attenuation coefficients in the crust of Japan and those in the continent of North America are close to each other.

Using these attenuation coefficients, the observed spectral amplitudes were equalized to a distance $r=100$ km and compared with the theoretical ones (the square root of the sum of Love and Rayleigh waves power spectra). The deviation of the observed spectra from the theoretical one should reflect the site amplification factor when the source effect and attenua-

Table 3. Attenuation coefficients at different periods.

period (sec)	α (km^{-1})	period (sec)	α (km^{-1})	period (sec)	α (km^{-1})
2	0.00322	7	0.00101	12	0.00046
3	0.00338	8	0.00076	13	0.00028
4	0.00249	9	0.00051	14	0.00023
5	0.00299	10	0.00051	15	0.00005
6	0.00230	11	0.00035	16	0.00002

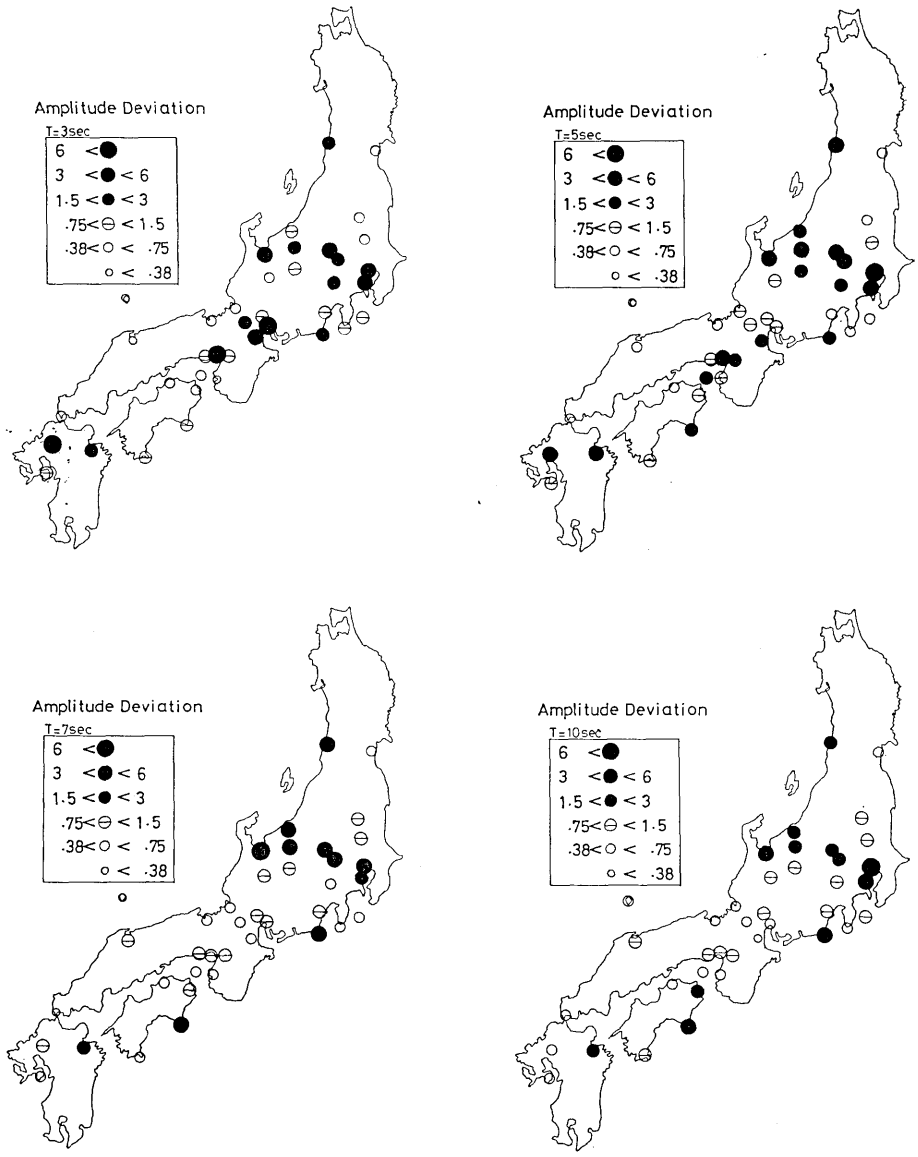

Fig. 8. Distribution of the ground-motion amplification factor at different periods, in Japan.

Table 4. Site amplification factors as a function of period, in Japan.

site \ period	3	4	5	6	7	8	9	10	11	12	13	14	15
Takayama	0.66	0.68	0.84	1.78	1.26	0.99	0.91	0.88	0.94	0.99	0.94	0.99	1.03
Gifu	1.13	1.21	1.41	0.98	0.77	0.69	0.75	0.83	0.91	1.07	1.23	1.38	1.50
Tsuruga	0.54	1.09	1.03	0.88	0.56	0.54	0.58	0.58	0.53	0.51	0.54	0.66	0.75
Toyama	5.83	5.02	3.52	5.69	8.01	11.13	8.53	5.10	4.53	5.56	6.14	6.10	5.74
Hikone	2.10	0.87	0.92	0.68	0.53	0.63	0.64	0.60	0.58	0.58	0.59	0.60	0.65
Nagoya	8.52	2.11	1.38	1.06	0.77	0.68	0.63	0.68	0.79	0.96	1.05	1.14	1.17
Matsumoto	0.82	1.49	1.52	3.39	1.46	1.45	1.48	1.43	1.54	1.70	1.64	1.60	1.35
Kameyama	3.39	2.24	1.54	1.26	0.38	0.62	0.47	0.36	0.37	0.59	0.82	0.96	1.03
Maizuru	0.44	0.49	0.50	0.38	0.38	0.43	0.44	0.42	0.40	0.43	0.46	0.51	0.55
Nagano	1.70	1.80	3.52	2.65	3.15	2.40	2.08	2.10	2.10	2.24	2.37	2.28	2.11
Nara	1.12	0.96	1.64	0.81	0.98	1.04	1.09	1.13	1.08	1.15	1.11	1.08	1.01
Takada	1.22	1.40	2.95	5.06	3.80	3.48	3.60	2.41	2.08	2.66	2.79	3.01	3.16
Osaka	14.57	10.03	3.41	1.78	0.83	0.61	0.57	1.03	1.19	1.22	1.34	1.65	1.96
Shizuoka	1.45	0.66	0.68	0.85	0.94	1.23	1.23	1.20	1.22	1.36	1.38	1.40	1.30
Funatsu	1.80	0.68	1.55	0.71	0.72	0.85	0.78	0.98	1.09	1.30	1.45	0.51	1.45
Kobe	1.19	1.37	1.45	1.42	1.04	1.18	1.28	1.28	1.14	1.11	1.07	1.14	1.22
Omaezaki	2.62	1.00	1.29	1.17	2.23	3.19	3.27	3.05	2.89	2.93	3.01	3.31	3.52
Maebashi	3.51	2.16	3.09	4.80	3.40	2.26	2.13	1.73	1.40	1.43	1.32	1.46	1.36
Kumagaya	2.65	1.44	4.31	5.14	4.06	3.49	3.51	2.02	1.66	2.65	3.07	3.47	2.77
Wakayama	0.26	0.45	0.98	0.97	0.70	0.66	0.60	0.58	0.75	0.94	0.94	0.98	1.04
Nagatsuro	1.10	0.38	0.54	0.89	0.73	0.67	0.68	0.69	0.68	0.82	0.94	1.05	1.11
Sumoto	0.62	1.20	1.62	0.65	0.50	0.58	0.55	0.73	0.78	0.77	0.70	0.64	0.60
Yokohama	3.53	2.67	4.31	3.36	2.28	1.91	2.49	3.35	3.89	5.00	6.51	7.10	6.82
Tokyo	3.21	2.32	9.59	14.40	5.90	8.65	11.18	13.88	11.94	11.01	11.99	11.42	9.82
Oshima	1.34	0.81	0.45	0.42	0.45	0.87	1.26	1.37	1.19	1.22	1.22	1.32	1.39
Utsunomiya	0.75	0.57	0.93	2.46	1.24	1.19	0.98	0.81	0.85	1.12	1.35	1.63	1.58
Tokushima	0.56	0.52	1.12	1.09	1.21	1.22	1.34	1.64	1.68	1.65	1.42	1.27	1.17
Saigo	0.27	0.39	0.17	0.42	0.18	0.18	0.22	0.49	1.09	2.28	2.93	3.32	3.29
Takamatsu	0.60	0.64	0.65	0.70	0.44	0.56	0.60	0.47	0.41	0.50	0.54	0.63	0.68
Yonago	0.23	0.28	0.41	0.79	0.89	0.97	0.81	1.21	1.57	2.06	2.47	2.63	2.49
Shirakawa	0.53	0.25	0.59	1.02	0.76	0.59	0.73	0.81	0.83	0.93	0.96	1.02	0.97
Murotomisaki	1.27	0.92	1.81	2.77	4.12	5.21	4.48	4.22	3.33	3.25	3.06	3.24	3.32
Sakata	2.54	1.91	3.88	4.01	4.44	4.09	2.70	2.55	3.36	4.41	4.33	4.29	3.92
Sendai	0.64	0.35	0.62	1.10	0.74	0.60	0.56	0.56	0.56	0.74	0.89	1.00	1.03
Shimizu	0.92	0.65	0.95	0.66	0.51	0.58	0.56	0.76	0.84	1.00	1.01	1.09	1.12
Oita	2.56	2.44	4.17	3.73	2.32	3.87	2.73	2.26	1.71	1.63	1.41	1.38	1.20
Shimonoseki	0.40	0.16	0.41	0.48	0.31	0.44	0.45	0.71	0.98	1.24	1.08	1.04	0.91
Saga	8.65	8.05	4.68	2.67	0.76	0.61	0.54	0.61	0.58	0.69	0.66	0.63	0.62
Unzendake	0.78	0.89	1.12	1.08	0.46	0.58	0.69	0.75	0.57	0.60	0.64	0.80	0.80

tion are excluded from the observations. These deviations, that is, the site amplification factors as a function of period are presented in Table 4. They are classified into 6 classes, as previously defined, and plotted on the maps (Fig. 8).

If one compares the results obtained by removing the source effect with those where the correction for source effect is not performed, the difference is apparent, as can be seen from Fig. 9. The significant difference (2 classes) in the values of site amplification factors at the period of 5 sec can be observed at Tokyo, Yokohama, Maebashi, Nagano, Takada, Sakata, Oita, etc.

Comparing our results at a period of 5 sec with Okada and Kagami's (Fig. 10), we can see that the patterns of site amplification factors closely resemble each other. Considering the instrumental response of JMA seismographs (T_0=5-6 sec) whose records were used in their analysis, it is reasonable to conclude that their results reflect the ground motion mainly at periods shorter than 6 sec. As these results are based on statistical analysis of large numbers of earthquakes, they give an average value. Therefore, the fact that the pattern of site amplification at a period of 5 sec in our results conforms with the results of Okada and Kagami leads us to the conclusion that the method introduced in this paper is satisfactory, even though the data from only one earthquake were used.

However, in a more detailed discussion, let us pay attention to the

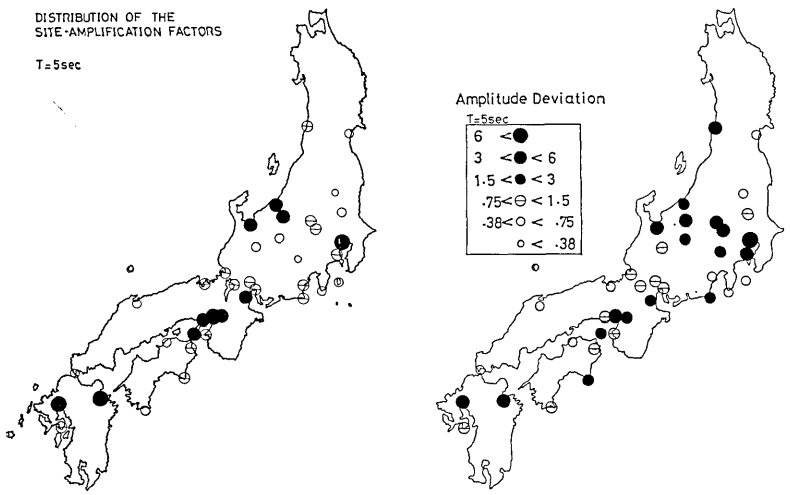

Fig. 9. Comparison of the apparent amplification factor of the observed data (a) and the amplification factor at the same site when the source effect is removed (b).

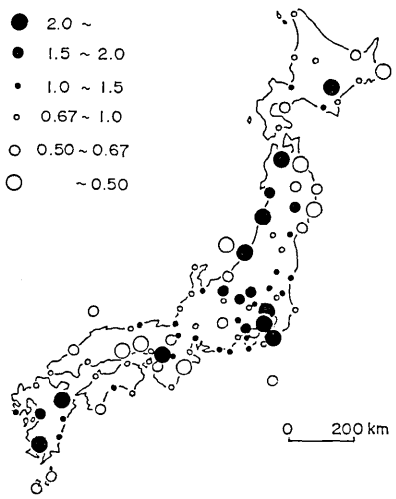

Fig. 10. Point-by-point amplitude amplification at long periods obtained by Okada and Kagami (1978).

following:

First, in the case of wide alluvial plains, such as the Kanto plain, the possible difference in the propagation paths, depending on the hypocenter location, should be considered. It would be necessary to determine the underground structure and analyse the data of more than one earthquake to obtain realistic results of site amplification factors.

Second, the sites where JMA instruments were located are not necessarily representative of the soil conditions at the area. To understand the shakeability at the construction site, the comparative observation and analysis of ground motion at the JMA instrument location and the site, are necessary.

Third, the spectra at long distances, e. g. Sakata and Miyazaki, are less precise than those at short distances because the digitization was not conducted for the late arrivals.

The final result—site amplification factors—presented in terms of classified shakeability, are plotted and shown in Fig. 11. At Osaka and Nagoya a high amplification is expected in periods of 3 sec to 4 sec, but a standard value should be expected at longer periods. In the case of Tokyo, however, a high amplification should occur at periods longer than 5 sec.

Concluding Remarks

In view of the possible damage to the long-period structures due to earthquake strong-motion, we proposed the method for determining the amplitude amplification factors at the given sites for different periods. As strong-motion data of the large number of earthquakes are still not readily available, the attempt is made to solve the problem by using a sufficiently large number of data from one earthquake, taking into account the source effect.

The deviation of the spectral amplitudes from the standard attenuation curve was determined for the observed values. The theoretical amplitudes were computed for the given source and underground stucture models and compared with the observed ones corrected by the epicentral

CLASS	1	2	3	4	5	6
AMPLITUDE FACTOR	≤ 0.38	0.38-0.75	0.75-1.5	1.5-3	3-6	≥ 6

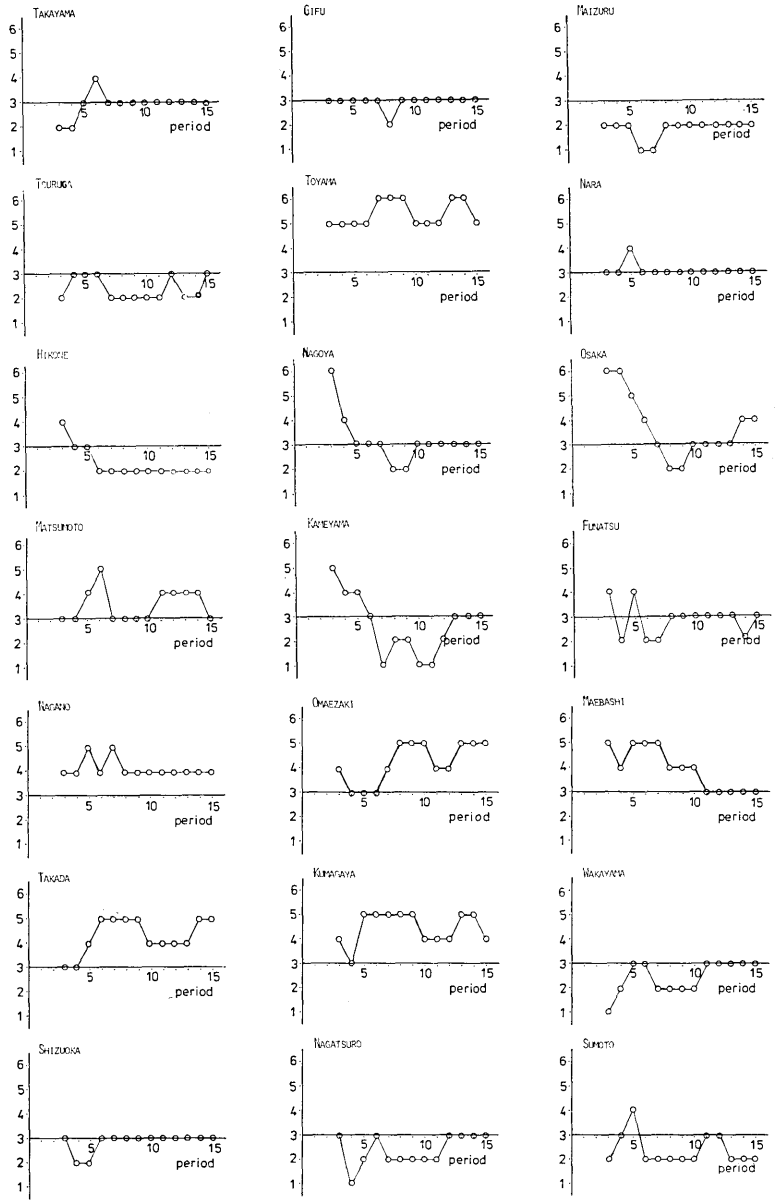

(a)

Fig. 11. Ground-motion amplification factors at the locations in terms of period.

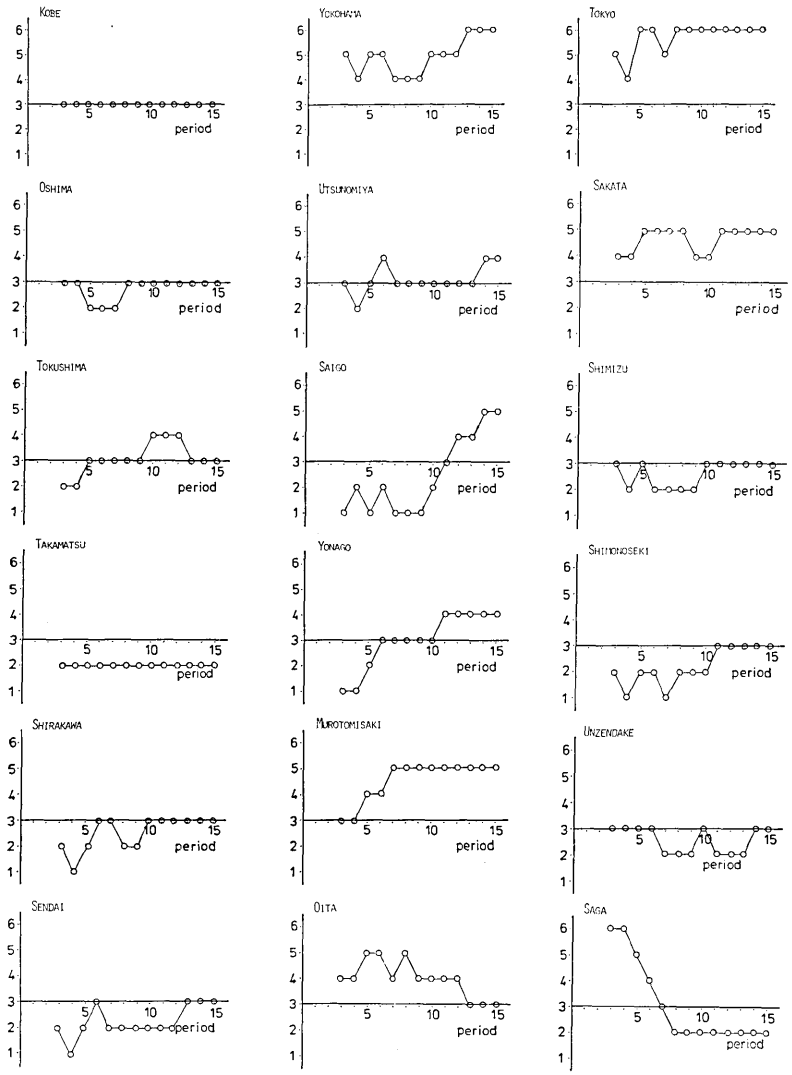

(b)

distance and attenuation coefficient. It is found that the site amplification factors deviate in a wide range and they depend strongly on period at some sites. The azimuthal variation of the observed waves depends on the source radiation pattern to the significant degree. The correction for a source effect yields the difference in the values of site factors up to 2 or even 3 times from the uncorrected ones. Finally, the site amplification factors sometimes differ more than 10 times from the standard value.

Seismic coefficients presently used for engineering purposes in mainland Japan are 0.8–1.0. According to our results, in the case of large earthquakes, this might not be a proper value, at least for long periods.

Acknowledgements

Prof. Y. Sato provided the digitized data of the Kita-Mino earthquake. Prof. R. Yoshiyama gave us many valuable comments on the Kita-Mino earthuake. Mr. Yanagisawa and members of the Earthquake Predication Center, E. R. I. especially Dr. Kohketsu, were helpful to Mamula. The authors are grateful to all of them. Mamula is indepted to the Kajima Gakujutsu Shinko Zaidan which supported her study in ERI.

References

CHENG, C. C. and B. J. MITCHELL, 1981, Crustal Q-structure in the United States from multi-mode surface waves, *Bull. Seis. Soc. Amer.*, **71**, 161–181.

HANKS, T. C., 1975, Strong ground motion of the San Fernando, California, earthquake: Ground displacement, *Bull. Seis. Soc. Amer.*, **65**, 193–225.

HARKRIDER, D. G., 1970, Surface waves in multilayered elastic media. Part II Higher mode spectra and spectral ratio from point sources in plain layered earth models, *Bull. Seis. Soc. Amer.*, **60**, 1937–1987.

HASEGAWA, H. S., 1974, Theoretical synthesis and analysis of strong-motion spectra of earthquake, *Can. Geotech. J.*, **11**, 278–298.

HERRMANN, R. B. and O. W. NUTTLI, 1975a, Ground motion modeling at regional distances for earthquakes in a continental interior, I. Theory and observations, *Earthq. Eng. Struct. Dyn.*, 4, 49–58.

HERRMANN, R. B. and O. W. NUTTLI, 1975b, Ground motion modeling at regional distances for earthquakes in a continental interior, II. Effect of focal depth azimuth and attenuation, *Earthq. Eng. Struct. Dyn.*, 4, 59–72.

HERRMANN, R. B., 1979, SH-wave generation by dislocation sources—a numerical study, *Bull. Seis. Soc. Amer.*, **69**, 1–16.

KAWASAKI, I., 1975, The focal process of the Kita-Mino earthquake of August 19, 1961 and its relationship to a quaternary fault, the Hatogayu—Koike Fault, *J. Phys. Earth*, 24, 227–250.

KAWASAKI, I., 1978, The near field Love-waves by exact ray method, *J. Phys. Earth*, 26, 211–237.

KUDO, K., S. ZAMA, M. YANAGISAWA and E. SHIMA, 1978, On the shear wave underground structure of Izu Peninsula, *Bull. Earthq. Res. Inst., Univ. Tokyo*, 53, 779–792.

KUDO, K., 1978, The contribution of Love waves to strong ground motions, *Proc. 2nd Inter. Conf. on Microzonation*, 2, 765–776.

KUDO, K., 1980, A study on the contribution of surface waves to strong ground motions, *Proc. 7th WCEE, Istanbul*, 2, 499–506.

KUDO, K. and M. SAKAUE, 1984, Oil-sloshing in the huge tanks at Niigata due to the Nihonkai-Chubu earthquake of 1983, *Bull. Earthq. Res. Inst., Univ., Tokyo*, 59, 361–382.

OHTA, Y. and Y. KAGAMI, 1976, Ultimate values of period and amplitude on seismic input motion in relation to a large-scale structure, *Bull. A.I.J.*, **249**, 53-60, (in Japanese).

OKADA, S. and Y. KAGAMI, 1978, A point-by-point evaluation of amplification characteristics in Japan on 1-10 sec seismic motion in relations to deep soil deposits, *Bull. A.I.J.*, **267**, (in Japanese).

SATÔ, Y. and E. SHIMA, 1978, Records and analysis of the Kita-Mino earthquake of August 19, 1961, Tokyo chokka zisin ni kansuru kenkyu, *Report of the Investigation Committee of Disaster Prevention of Tokyo Metropolis*, **6**, 91-117, (in Japanese).

SWANGER, H.J. and D.M. BOORE, 1978a, Simulation of strong-motion displacement using surface wave modal superposition, *Bull. Seis. Soc. Amer.*, **68**, 907-922.

SWANGER, H.J. and D.M. BOORE, 1978b, Importance of surface waves in strong ground motion in the period range of 1 to 10sec, *Proc. 2nd Intern. Conf. on Microzonation*, **3**, 1447-1469.

TRIFUNAC, M.D. and J.N. BRUNE, 1970, Complexity of energy release during the Imperial Valley, California, earthquake of 1940, *Bull. Seis. Soc. Amer.*, **60**, 137-160.

Appendix I. JMA Strong-Motion Displacement Records of the Kita-Mino Earthquake of August 19, 1961.

Appendix I-1.

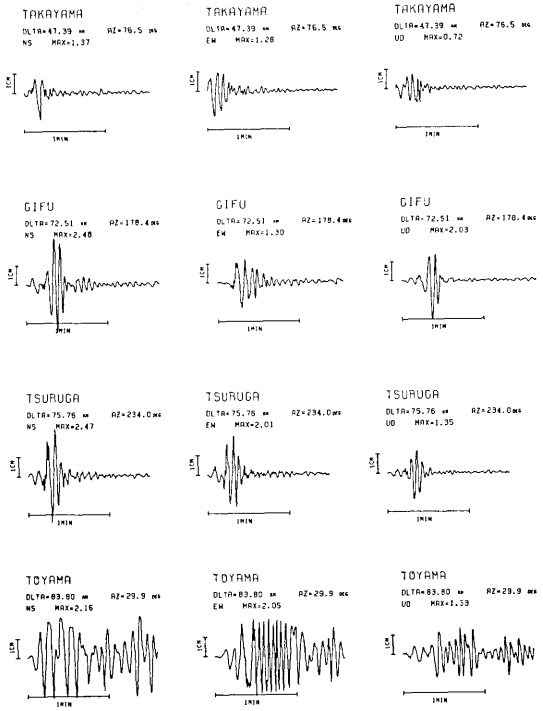

Appendix I-2.

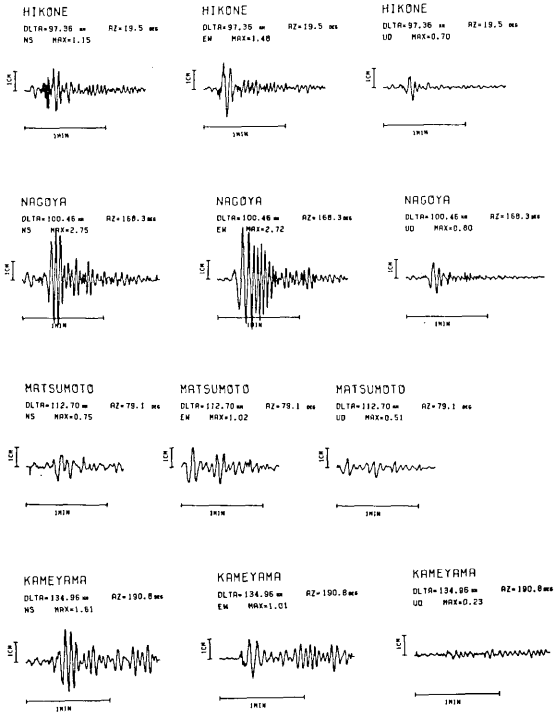

Appendix I-3.

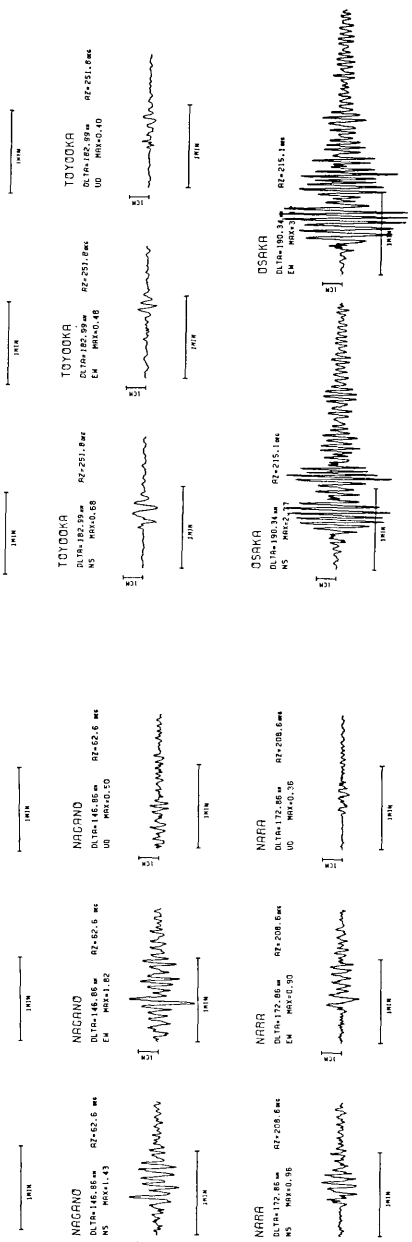

Appendix I-4.

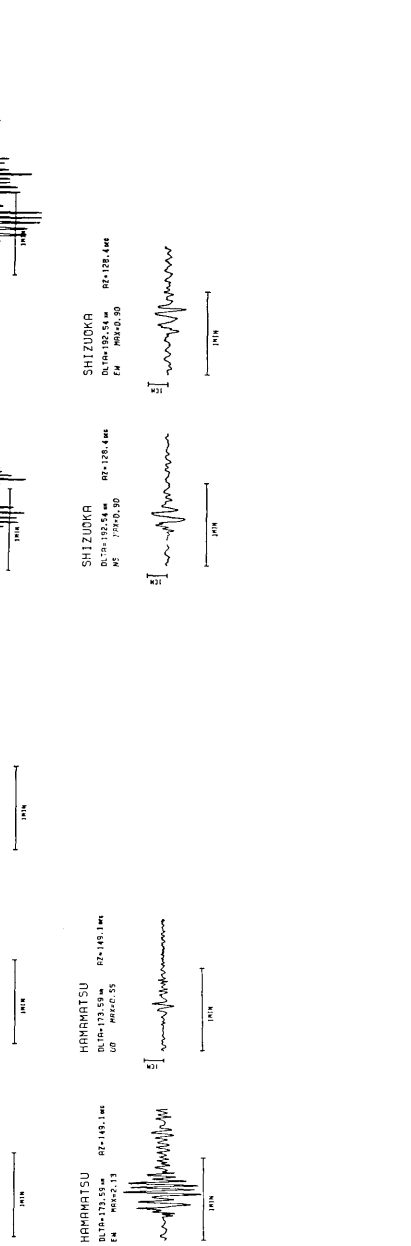

Appendix I-5.

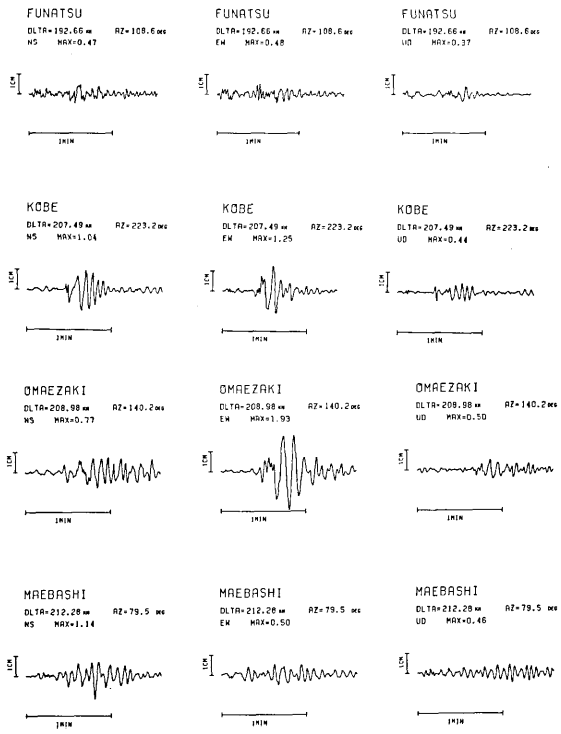

Appendix I-6.

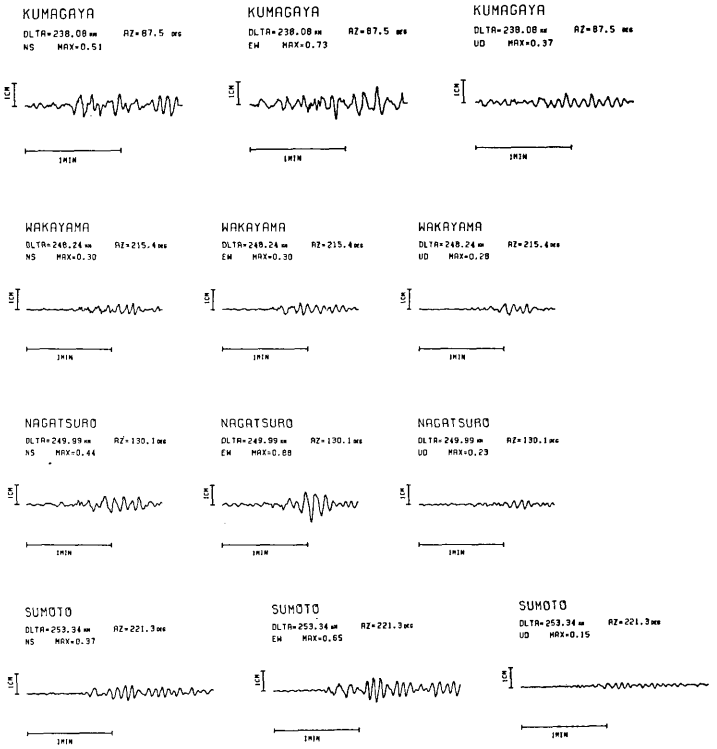

Appendix I-7.

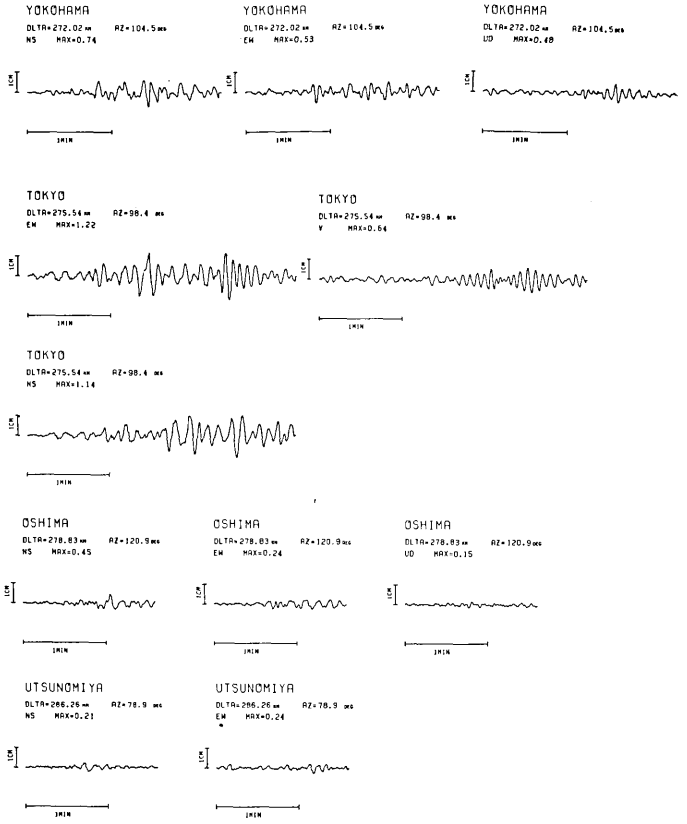

Appendix I-8.

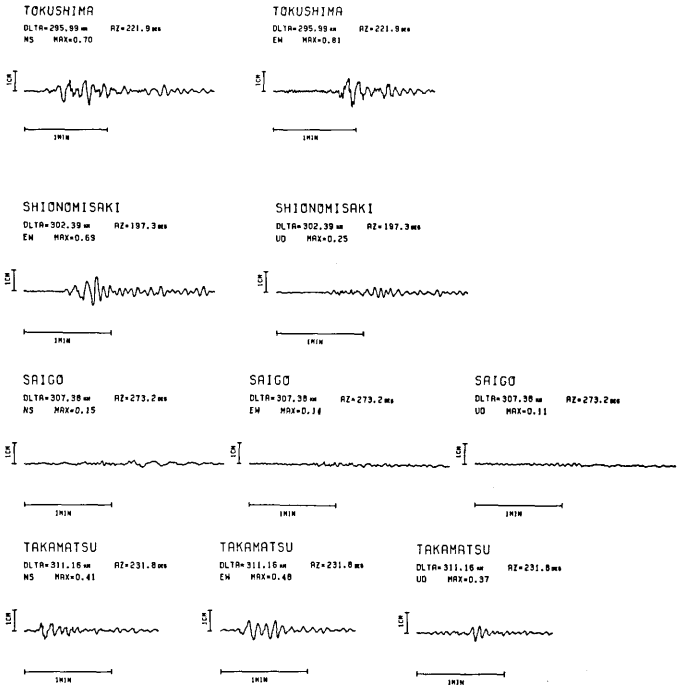

Appendix I-9.

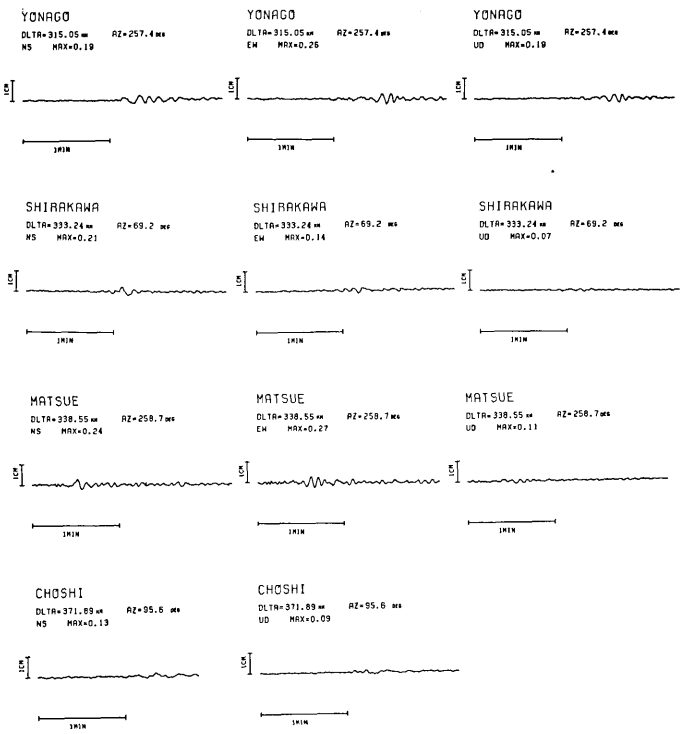

Appendix I-10.

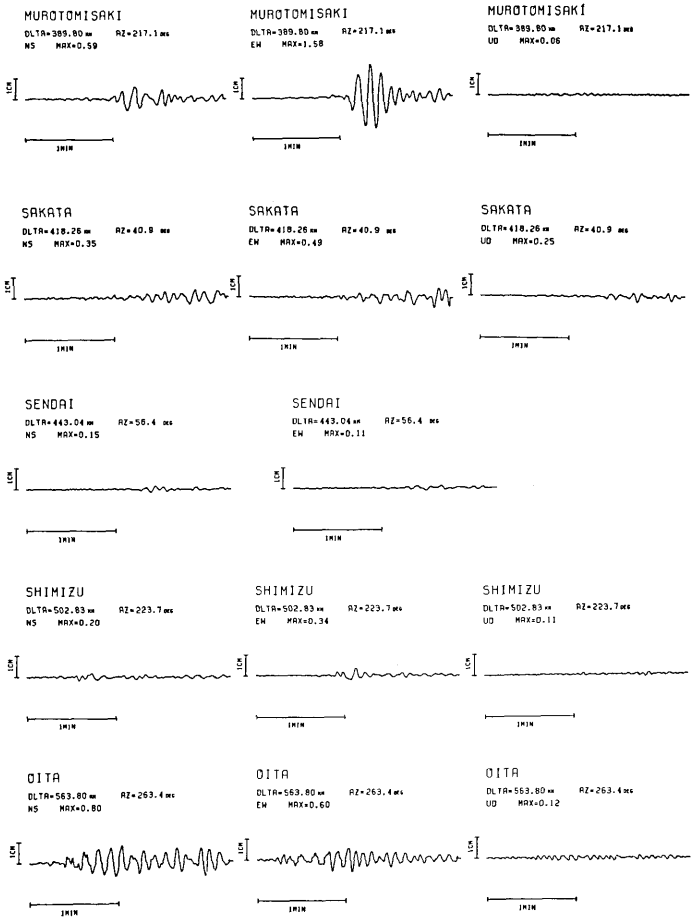

Appendix I-11.

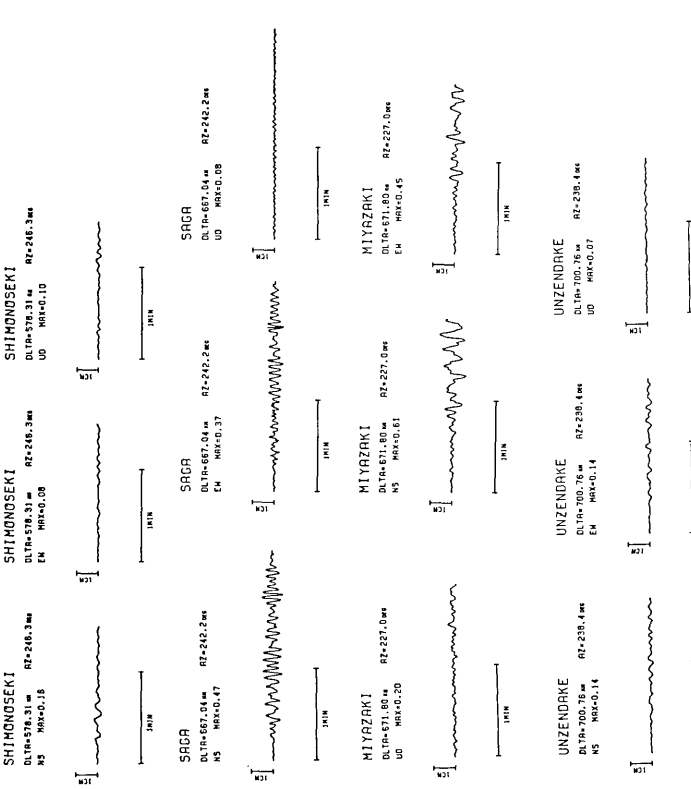

Appendix II. Fourier Spectral Amplitudes of the JMA Strong-Motion Records of the Kita-Mino Earthquake, August 19, 1961. The instrumental response was removed.

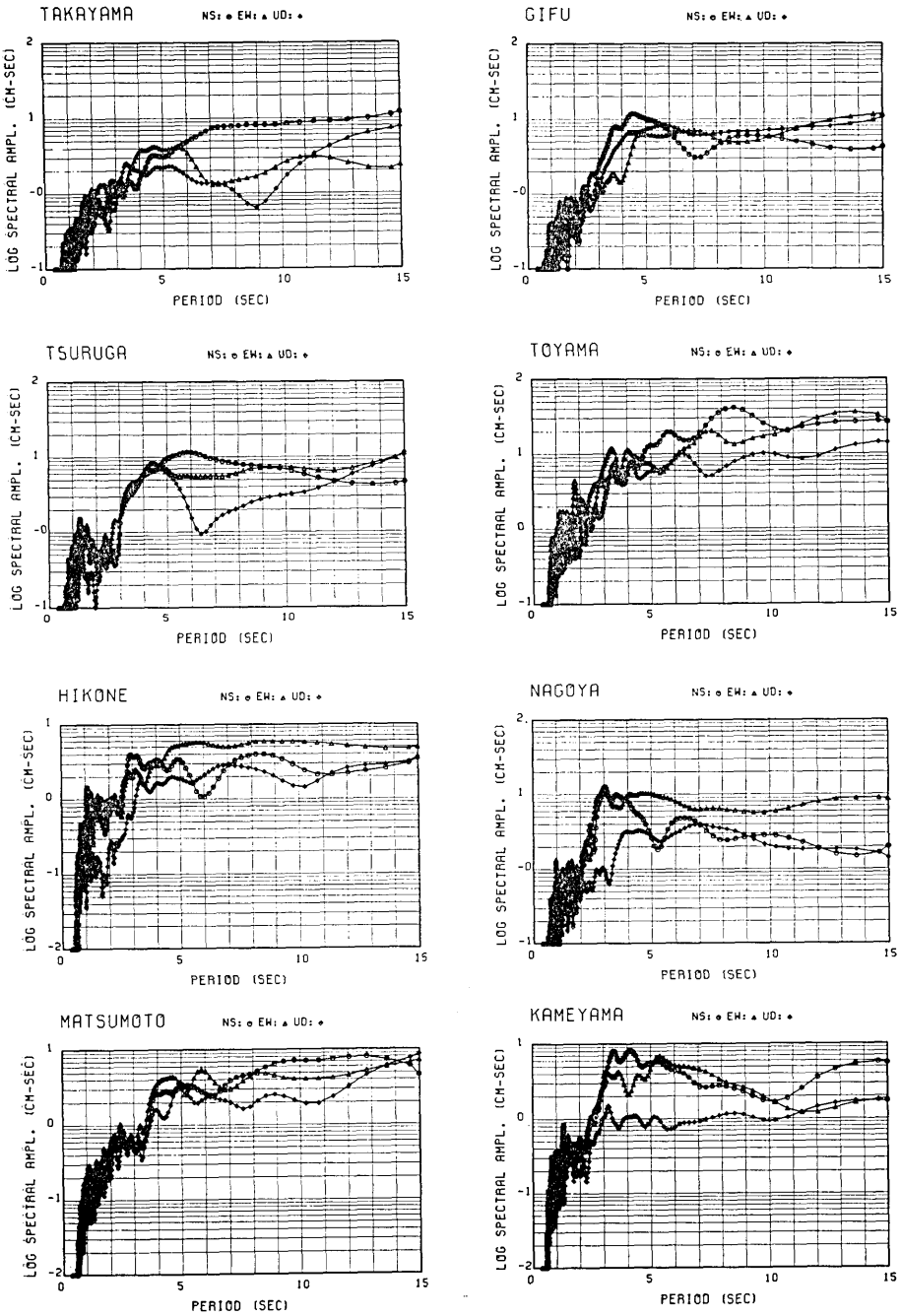

Appendix II-2.

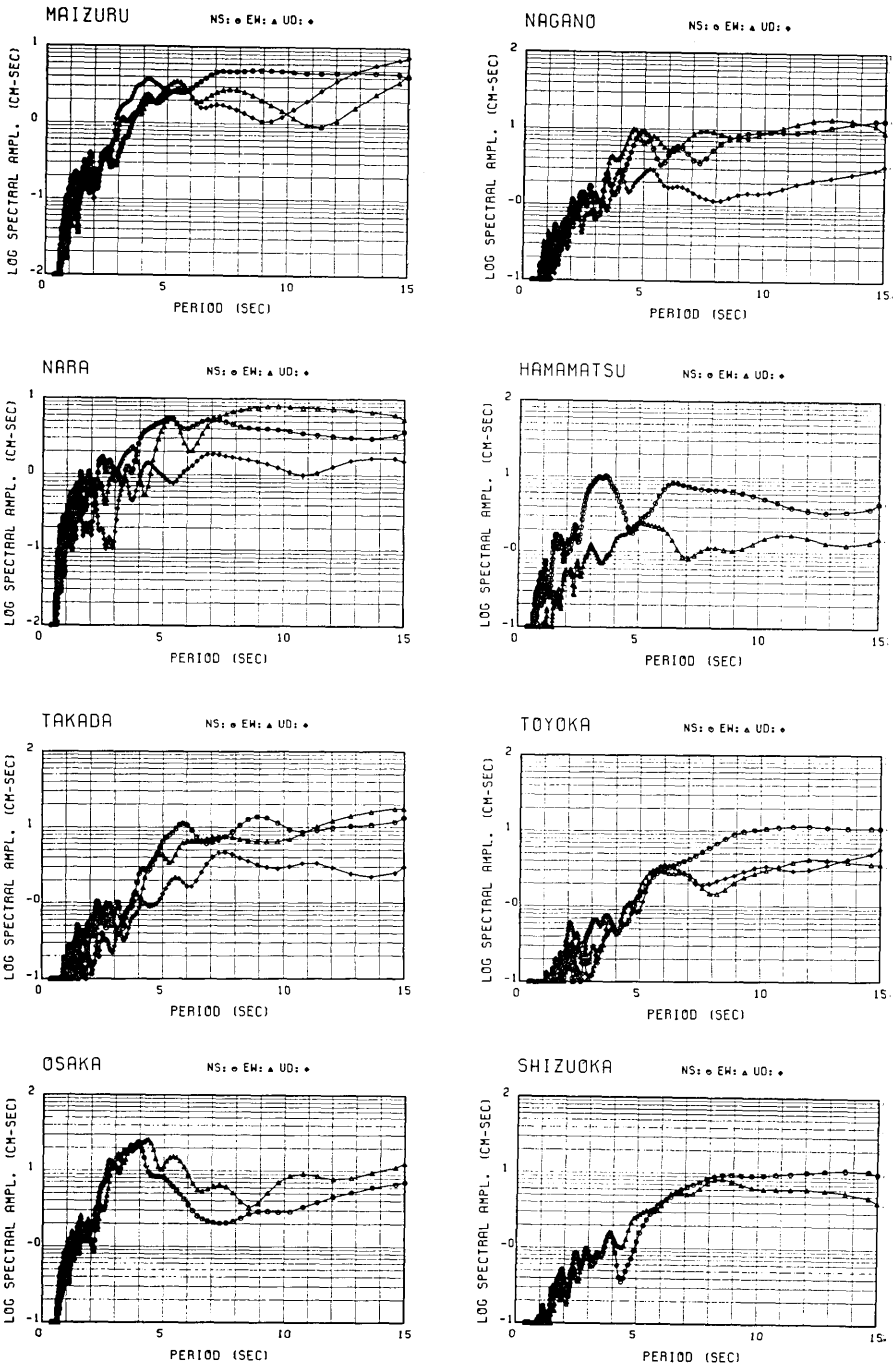

Appendix II-3.

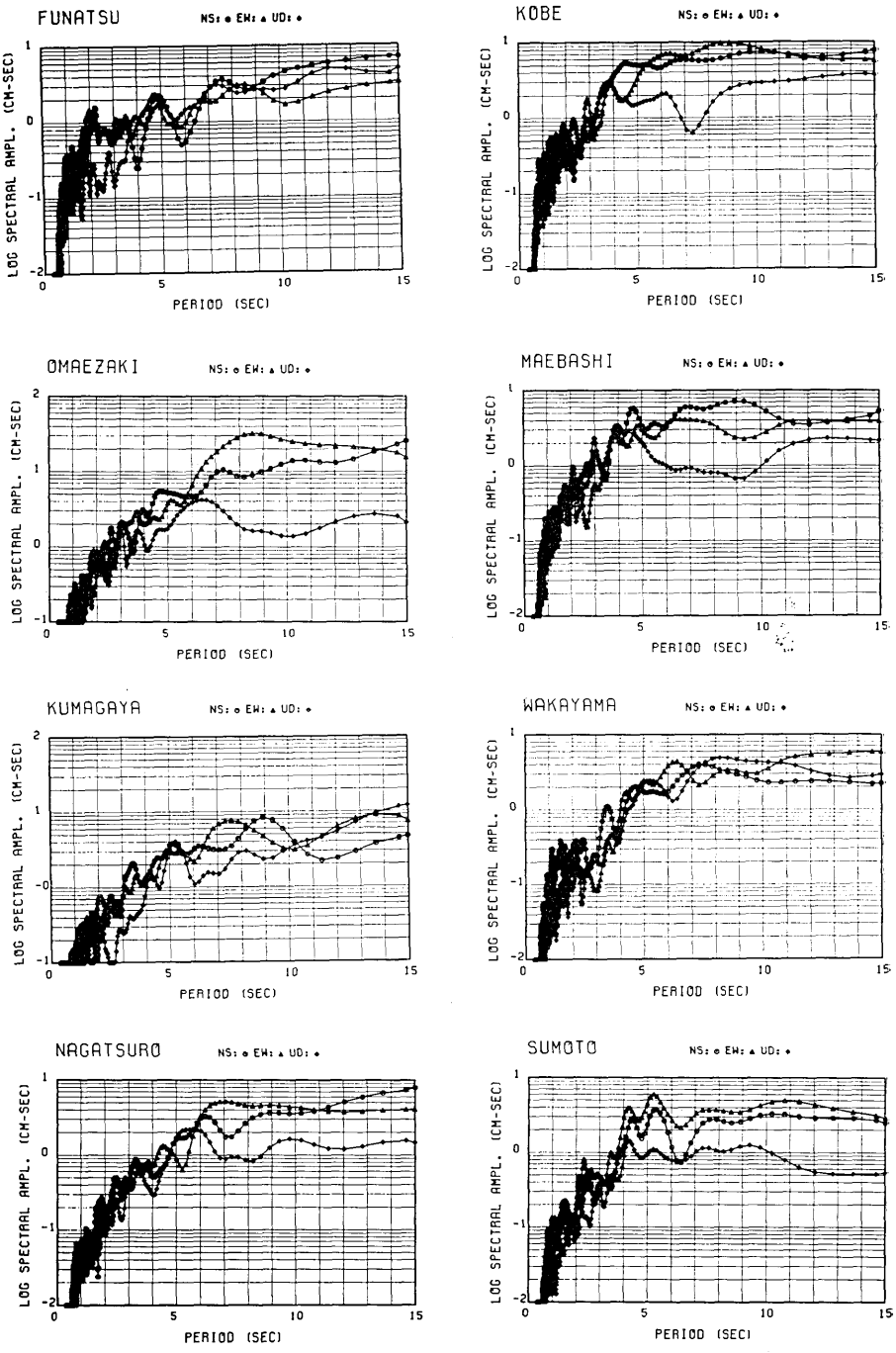

Appendix II-4.

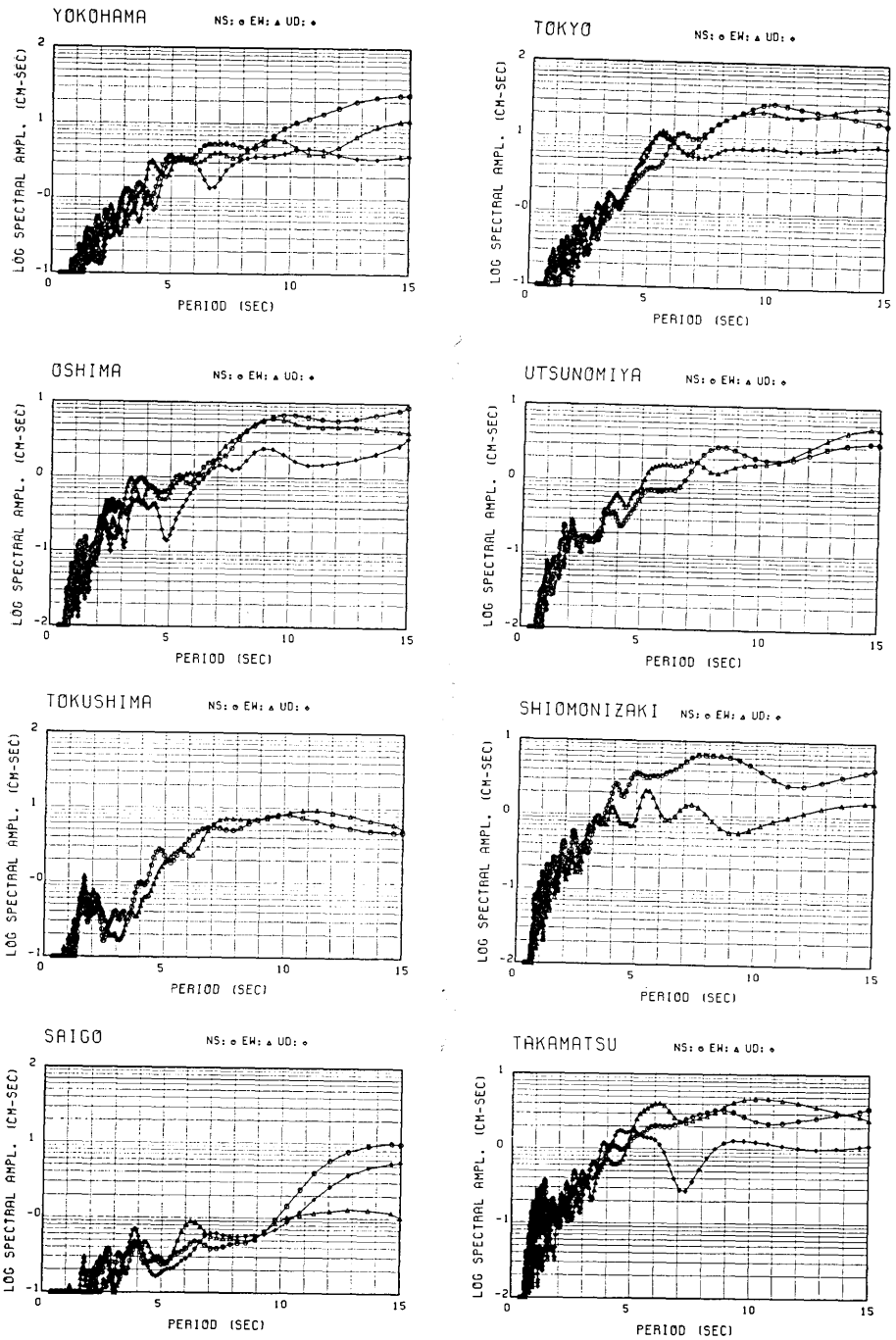

Appendix II-5.

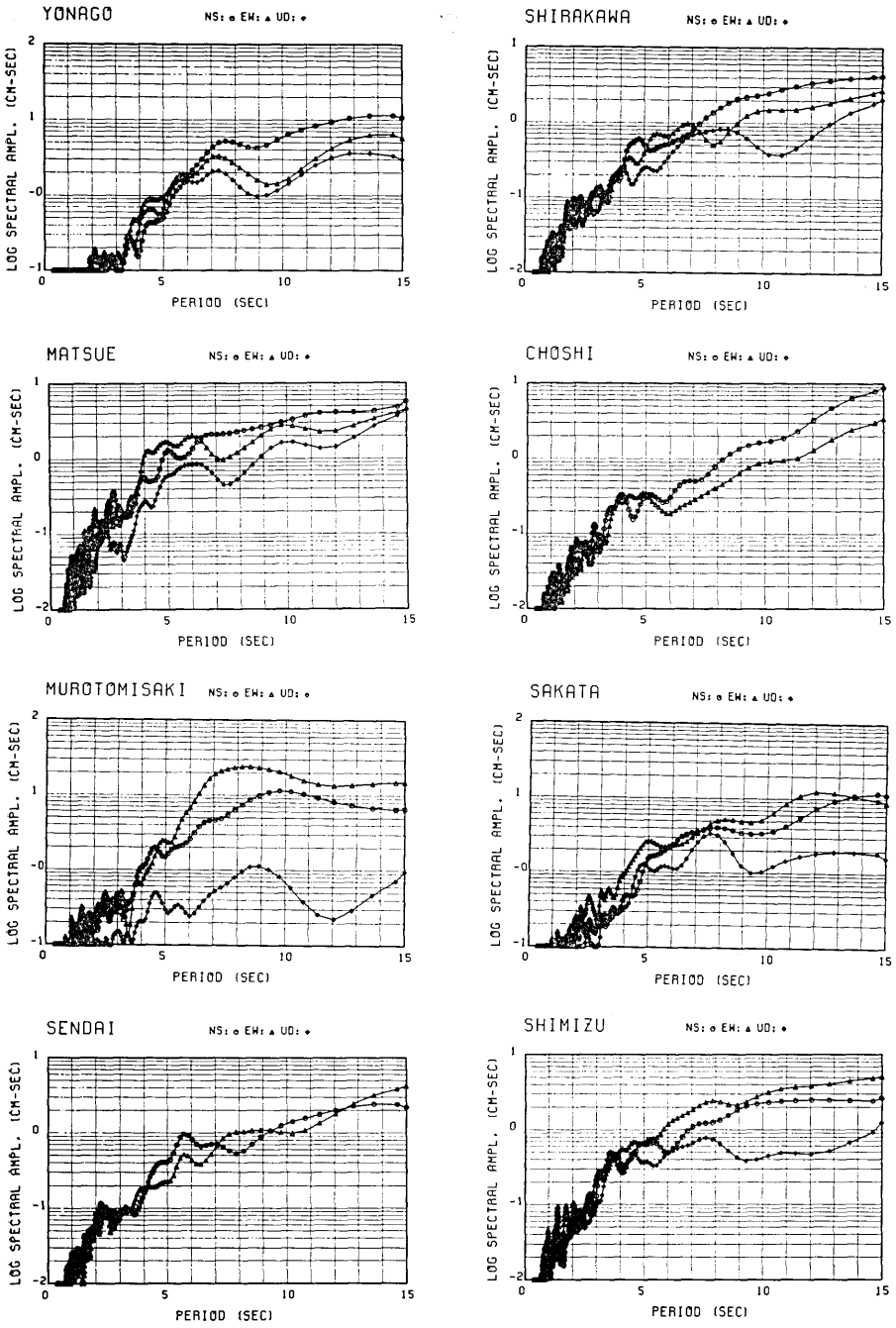

Appendix II-6.

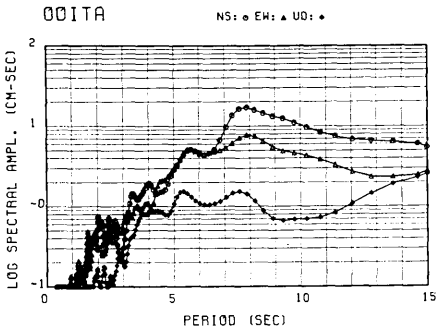

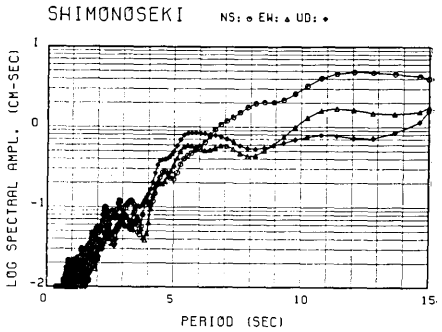

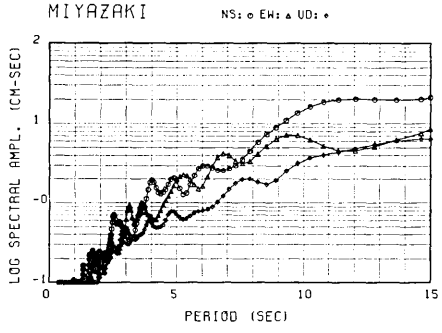

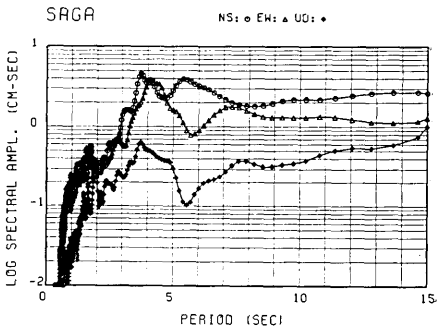

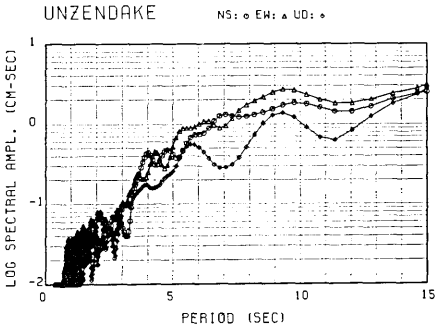

周期特性 (3-15秒) を考慮した日本各地における地震動の増幅度分布

地震研究所 { マムラ，リュビツァ / 工藤一嘉 / 嶋悦三

固有周期が数秒から10数秒に至る長周期構造物，例えば大型石油タンク，長大橋，高層ビル等は年々増加の傾向をたどっている．しかし，これらの構造物の耐震安全性を検討する際に，基礎資料となる長周期の地震動の性質については，十分把握されているとは言い難い面がある．加速度記録の解析を通じ，地震動の平均像あるいは地盤での増幅特性に関する研究から，短周期地震動に対する知見は比較的多いが，上記の周期帯に関してはこの限りではない．一方，断層モデルによる地震動の解釈は徐々に短周期領域にまで拡張され，地震の大きさにも依るが，周期 2～3 秒以上の地震動に関してはほぼ決定論的に説明されるようになってきた．従って，地震学においてはこれ等の周期帯の問題も既に解決ずみであるとの考え方もある．しかしながら工学への応用に至る段階では，多くの解決されるべき問題が残されている．その1つに地震動の地域特性があげられよう．岡田・鏡味 (1978) は気象庁1倍強震計記録の最大振幅を利用し，日本各地における地震動の揺れ易さ，揺れにくさの地域分布を求めた．最も揺れにくい地点（尾鷲）と，最も揺れ易い地点（酒田）とでは，10倍強の差が指摘されている．但し，彼等の結果は最大振幅のみを利用しているため，周期特性は必ずしも明瞭ではない．長周期構造物は一般に減衰が小さく，入力地震動に対する周期の選択性が著しい．従って耐震設計資料としては地震動のスペクトル特性がより重要となる．

我々は全国の揺れ易さ，揺れにくさを周期の関数として表現することを試みた．記録の数値化から始まるこの作業においては，岡田・鏡味 (1978) のように多くの地震を解析することは労力・時間が膨大となる．そこで，少数の地震に対し，広く観測記録が得られている場合を扱うことでこの問題の解決を試みた．ここでは1961年北美濃地震 (M=7.0) の気象庁1倍強震計記録を用いた．記録の数値化は河角によって実施され，佐藤・嶋 (1978) によって修正・整理された．

各地点のスペクトルとして，正確さは欠くが，南北および東西動成分のそれぞれの自乗和の平方根を用い，上下動成分を省略する簡単化を行なった．震源が浅いことから，距離減衰の関数形として，$A(\omega)=A_0\exp(-\alpha r)/\sqrt{r}$ を仮定した（A_0=常数，ω=角周波数，α=減衰係数，r=震央距離）．Fig. 3 は周期毎に求めた減衰曲線であるが，距離補正後のスペクトルをプロットしてあるため，図に示された平均線の傾きは減衰係数を与えている．平均値からのずれがその地点における揺れ易さ，揺れにくさの指標となる．しかし，地震動は震源による方位特性を受けたものであり，地域特性のみを抽出するためには，これを取り除く必要がある．

震源モデル・標準的地下構造モデルを確定するため，震源をとりまく点，高山・岐阜・敦賀における地震動を正規モード解により合成し，観測記録と比較した．その結果，KAWASAKI (1975) による断層モデルを若干修正し，標準構造として Table 2 に示すモデルを用いることにより，観測値と合成波の調和を見た (Fig. 5, 6)．従って上記モデルを用いた合成スペクトルは，震源の方位特性を含めた標準値を与える．平均値から3倍以上および1/3以下のデータを除き減衰係数を再決定し(Table 3)，観測値を減衰なしの値に引き直した．補正した観測スペクトルと合成スペクトル (Rayleigh 波と Love 波) の比は地域増幅度を与える．

最終的に，周期の関数としての地域増幅度は Fig. 8, Table. 4 のように求まった．沖積平野が発達している地域で振幅が大きくなる傾向を示し，かなりの数の地域で周期によって著しく振幅が変化している (Fig. 11)．

大阪を例にとれば，周期5秒以下では平均の10倍に達するが，7秒以下になれば全国平均になる．このような地域では構造物種別の選定が重要な課題となろう．また耐震設計に用いられる地域係数には多くの問題が含まれていると考えられる．例えば石油タンクの耐震規定にもり込まれている地域係数は 0.8～1.0 とされ，短周期地動に対するものと同等であるが，このような小さな地域差では現実

を評価できないことは明白である．揺れにくい地域では地震動を過大評価し経済的損失を招き，一方では揺れやすい地域では耐震安全性が問題となる．

工学への実用化を目ざすためには，残された地域での評価，さらに幾つかの地震に対し同種の解析を行ない各地点での平均像を求めること等が必要であろう．また観測記録の得られた地点が必ずしもその地域を代表する地盤条件にあるとは限らない．従って建設サイトと観測地点（気象庁官署）との相対的地震動特性を見い出すことも重要となろう．